Optics Letters

Graded-index solitons in multimode fibers

AMIRA S. AHSAN* AND GOVIND P. AGRAWAL

The Institute of Optics, University of Rochester, Rochester, New York 14627, USA
*Corresponding author: aahsan@ur.rochester.edu

Received 17 May 2018; revised 15 June 2018; accepted 16 June 2018; posted 18 June 2018 (Doc. ID 331852); published 10 July 2018

We investigate stability of optical solitons in graded-index (GRIN) fibers by solving an effective nonlinear Schrödinger equation that includes spatial self-imaging effects through a length-dependent nonlinear parameter. We show that this equation can be reduced to the standard NLS equation for optical pulses whose dispersion length is much longer than the self-imaging period of the GRIN fiber. Numerical simulations are used to reveal that fundamental GRIN solitons as short as 100 fs can form and remain stable over distances exceeding 1 km. Higher-order solitons can also form, but they propagate stably over shorter distances. We also discuss the impact of third-order dispersion on a GRIN soliton.

OCIS codes: (190.4370) Nonlinear optics, fibers; (190.5530) Pulse propagation and temporal solitons.

https://doi.org/10.1364/OL.43.003345

Temporal solitons have been studied extensively in the context of single-mode optical fibers [1–3]. The question of whether solitons can form inside multimode fibers attracted attention as early as 1980 [4,5]. It was realized that different group delays associated with different modes were likely to hinder the formation of such solitons. Since intermodal group delays are much smaller inside a graded-index (GRIN) nonlinear medium, it was natural to consider the formation of multimode solitons in a GRIN medium. Indeed, theoretical work during the 1990 s indicated that a GRIN medium may even support the formation of spatiotemporal solitons that are confined in both space and time [6,7]. Although such bullet-like solitons have not yet been observed, a multimode temporal soliton composed of three modes was observed in 2013 inside a GRIN fiber [8]. Since then, multimode solitons have remained of continuing interest [9–11].

Two approaches have been used to model multimode solitons. In a brute-force technique, the full four-dimensional [$(3+1)D$] problem is solved numerically, with different approximations made to manage the computing time [8,9]. Alternatively, a modal expansion is made, and a large set of coupled $(1+1)D$ nonlinear Schrödinger (NLS) equations are solved numerically [9,12]. Both techniques require substantial computational resources. Here we employ a much simpler approach in which a single NLS equation is used to study the formation of GRIN solitons. This equation was derived recently [13] using the variational solution obtained in 1992 for a Gaussian beam propagating inside a GRIN medium [14]. The periodic self-imaging of a Gaussian beam results in a NLS equation whose nonlinear term varies periodically along the length of a GRIN fiber. The same periodic behavior applies to all beams that represent nonlinear eigenmodes of the spatial problem [15]. We use the $(1+1)D$ NLS equation to investigate the conditions under which temporal solitons can form inside a GRIN fiber.

Since the full problem is quite involved, it is important to make some simplifications. We assume that a pulsed Gaussian beam is propagating along a GRIN fiber whose refractive index varies inside the core as

$$n(\mathbf{r}, I) = n_0(\omega)[1 - \Delta(\rho/a)^2] + n_2 I(\rho \leq a), \tag{1}$$

where n_0 is the core index, a is the core radius, $\Delta = (n_0 - n_c)/n_0$, n_c being the cladding index. The last term represents self-focusing, and it depends on the local intensity I and the Kerr coefficient n_2. We ignore the cladding completely and assume that the beam remains confined to the fiber core because of the graded nature of the refractive index and the Kerr self-focusing. We also neglect all polarization effects and assume that the electric field is polarized along the x axis and that this state of polarization does not change with propagation.

Using $\mathbf{E}(\mathbf{r}, t) = \hat{\mathbf{x}} E(\mathbf{r}) e^{i\beta_0 z - i\omega_0 t}$ with $\beta_0 = n_0\omega_0/c$ at the carrier frequency ω_0, and assuming $E(\mathbf{r})$ to be a slowly varying function of z, the full $(3+1)D$ propagation equation is [13]

$$i\frac{\partial E}{\partial z} + \frac{1}{2\beta_0}\nabla_T^2 E + \hat{D}\left(i\frac{\partial}{\partial t}\right)E - \beta_0\Delta\frac{\rho^2}{a^2}E + \frac{n_2\omega_0}{c}|E|^2 E = 0, \tag{2}$$

where ∇_T^2 is the transverse Laplacian operator and $\hat{D}$ is the dispersion operator in the form $\hat{D}(\omega) = \sum_{m=2}\beta_m\omega^m/m!$ [3]. If only group-velocity dispersion (GVD) is included, $\hat{D}(\omega) = \beta_2\omega^2/2$, where β_2 is the GVD parameter. A numerical solution of the preceding equation is time-consuming because of its $(3+1)D$ nature.

Conforti *et al.* [13] used the known Gaussian beam solution obtained in 1992 in the form [14]

$$F(\mathbf{r}) = \frac{w_0}{w}\exp\left[-\frac{(x^2+y^2)}{2w^2} + i\phi(\mathbf{r})\right], \tag{3}$$

to write the solution of Eq. (2) as $E(\mathbf{r}, t) = A(z, t)F(\mathbf{r})$ and showed that $A(z, t)$ satisfies the $(1+1)D$ NLS equation

$$i\frac{\partial A}{\partial z} - \frac{\beta_2}{2}\frac{\partial^2 A}{\partial t^2} + \gamma f^{-1}(z)|A|^2 A = 0, \tag{4}$$

where the nonlinear parameter $\gamma = \omega_0 n_2/(cA_{\text{eff}})$ is defined using the effective area of the input Gaussian beam and the periodically varying function $f(z)$ is given by

$$f(z) = w^2(z)/w_0^2 = \cos^2(\pi z/z_p) + C\sin^2(\pi z/z_p). \tag{5}$$

Here w_0 is the input beam width, and the parameters z_p and C are defined as

$$z_p = \frac{\pi a}{\sqrt{2\Delta}}, \quad C = \frac{(1-p)z_p^2}{(\pi\beta_0 w_0^2)^2}, \tag{6}$$

where p is related to the input peak power P_0 as $p = n_2(\beta_0 w_0)^2 P_0/2n_0$. Physically, z_p is the self-imaging period of a GRIN fiber, indicating that the beam width w oscillates such that it recovers its input value w_0 at distances that are multiples of z_p. At distances $z = m(z_p/2)$, w/w_0 takes its minimum value $\sqrt{C}$, i.e., C governs the extent of beam compression during each cycle. The Kerr nonlinearity affects C through the dimensionless number p that is related to the beam collapse known to occur in any nonlinear Kerr medium for $p = 1$. Multimode solitons discussed here require much lower peak powers ($p \ll 1$). The phase $\phi(\mathbf{r})$ appearing in Eq. (3) is given in Ref. [14], but its explicit form is not needed in this work.

Equation (4) includes the impact of spatial beam width oscillations of a Gaussian beam resulting from GRIN-induced self-imaging through the function $f(z)$. It reduces a complex $(3+1)D$ problem to a single NLS equation that is much faster to solve and can be used to gain physical insight.

We now investigate under what conditions Eq. (4) can support GRIN solitons whose temporal shape does not change along the fiber length. It is clear from the presence of $f(z)$ in this equation that standard temporal solitons studied in the context of single-mode fibers [3] cannot form in GRIN fibers. More precisely, this equation is not integrable by the inverse scattering method, which rules out the formation of ideal solitons. However, an equation similar to Eq. (4) has been found before in the context of long fiber links employing amplifiers periodically for compensating fiber losses. It was found in 1990 that a new kind of soliton, known as the guiding-center soliton, can propagate inside such fiber links [16]. It is also known as the loss-managed soliton [17]. Under appropriate conditions, such a soliton should also exist in GRIN fibers. We refer to it as the GRIN soliton to emphasize that a parabolic index profile is essential for its existence.

It is useful to normalize Eq. (4) in soliton units using [3]

$$\tau = t/T_0, \quad \xi = z/L_D, \quad U = A/\sqrt{P_0}, \tag{7}$$

where T_0 and P_0 are the width and the peak power of input pulses, and $L_D = T_0^2/|\beta_2|$ is the dispersion length. The normalized NLS equation then takes the form

$$i\frac{\partial U}{\partial \xi} + \frac{1}{2}\frac{\partial^2 U}{\partial \tau^2} + N^2 f^{-1}(\xi)|U|^2 U = 0, \tag{8}$$

where we assumed anomalous GVD ($\beta_2 < 0$) and introduced the soliton order N through $N^2 = \gamma P_0 L_D$. Using Eq. (4), the periodic function $f(\xi)$ can be written as

$$f(\xi) = \cos^2(\pi q\xi) + C\sin^2(\pi q\xi), \quad q = L_D/z_p. \tag{9}$$

For typical GRIN fibers with $a = 25$ μm and $\Delta = 0.01$, the self-imaging period z_p is a fraction of 1 mm. In contrast, the dispersion length L_D for a fiber exceeds 50 cm for $T_0 > 0.1$ ps (using $\beta_2 = -20$ ps^2/km at wavelengths near 1550 nm). As a result, q is a large number with values $q > 100$ even for relatively short 200 fs input pulses. Thus, the beam width inside a GRIN fiber oscillates hundreds of times within one dispersion length in most practical situations.

As discussed in Ref. [16], the dispersion length provides the scale over which solitons evolve. Since solitons cannot respond to beam width changes taking place on a scale of 1 mm or less, their temporal width does not change much even when the spatial width changes by a large fraction. This feature suggests that a soliton-like evolution of optical pulses is possible inside GRIN fibers, in agreement with recent observations [8]. We can find the input power needed for launching such GRIN solitons by writing the solution of Eq. (8) in the form $U = \bar{U} + u$, where $\bar{U}$ represents average over one period z_p. The fast-scale perturbations can be shown to satisfy $|u| \ll |\bar{U}|$ as long as $q \gg 1$ [16]. The average soliton dynamics are captured by the NLS equation

$$i\frac{\partial \bar{U}}{\partial \xi} + \frac{1}{2}\frac{\partial^2 \bar{U}}{\partial \tau^2} + i\bar{N}^2|\bar{U}|^2\bar{U} = 0, \tag{10}$$

where $\bar{N}$ is defined by averaging the nonlinear term average over the self-imaging period z_p as

$$\bar{N}^2 = N^2\frac{1}{z_p}\int_0^{z_p} f^{-1}(z)\mathrm{d}z = \frac{N^2}{\sqrt{C}}, \tag{11}$$

where the integration was carried out using $f(z)$ given in Eq. (5). This is our main result. It shows that the peak power of input pulses must be adjusted to ensure $\bar{N} = 1$ for the fundamental GRIN solitons. From the preceding equation, this can be realized if we choose $N^2 = \sqrt{C}$. Since $N^2 = \gamma P_0 L_D$, the peak power P_0 of input pulses must be reduced by the factor of $\sqrt{C}$ to realize GRIN solitons. This makes sense physically by noting that a reduction in the spatial beam width during each self-imaging cycle enhances the peak power of pulses. This enhancement must be balanced, on average, by reducing the input power by an appropriate factor.

Since Eq. (8) is not exactly integrable, it follows that the GRIN solitons, representing solutions of Eq. (10), may not be absolutely stable. The important question is over what distances such solitons propagate stably. To answer this question, we solve Eq. (8) numerically so that all perturbations induced by beam width oscillations are automatically included. We choose $C = 0.2$ for which beam width is reduced by a factor of about 2.2 during each cycle. The input field is taken in the form $u(0,\tau) = \text{sech}(\tau)$ and $N = C^{1/4}$ to ensure it forms a fundamental GRIN soliton. Figure 1 shows the evolution in two cases of (a) $q = 100$ and (b) $q = 1$. As expected, the soliton maintains both its shape and spectrum over $100L_D$ for a large value of q. We compare the shape and spectrum at $100L_D$ to those at the input end in Fig. 2(a). All perturbations induced by beam width oscillations remain negligible (below a 50 dB level) even after 100 dispersion lengths. Since dispersion length can exceed 50 m for pulses longer than 1 ps, such solitons should remain intact over fiber lengths exceeding 10 km. By the same token, 100 fs GRIN soliton can survive over 100 m.

The $q = 1$ case shown in Fig. 1(b) corresponds to the worst-case scenario since the dispersion length is equal to the

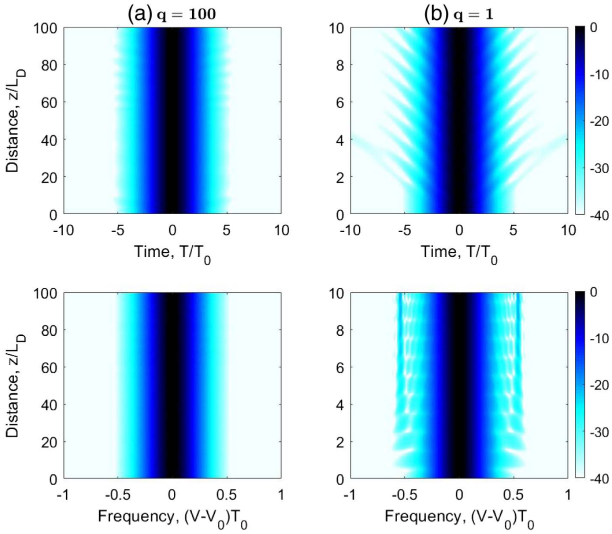

Fig. 1. Temporal (top) and spectral (bottom) evolutions of the fundamental GRIN soliton using $C = 0.2$. (a) Evolution over $100L_D$ for $q = 100$; (b) evolution over $10L_D$ for $q = 1$. In both cases, intensity is color coded on a 40 dB scale.

self-imaging distance. This may happen in practice for ultrashort pulses ($L_D = 5$ mm for $T_0 = 10$ fs). Although GRIN solitons are not stable in this limiting case, their evolution over $10L_D$ still remains acceptable. As seen in Fig. 2(b), the pulse shape remains sech-like, and perturbations induced by beam width oscillations remain at the 40 dB level after $10L_D$. The spectrum now exhibits sidebands, but their amplitude is still below 1%.

The preceding results assumed $C = 0.2$, and one may wonder how they change if C is different. We have carried out numerical simulations for values of C in the range 0.1–10 and found no qualitative differences. Notice that $C = 1$ is a special case in which the beam width remains constant with

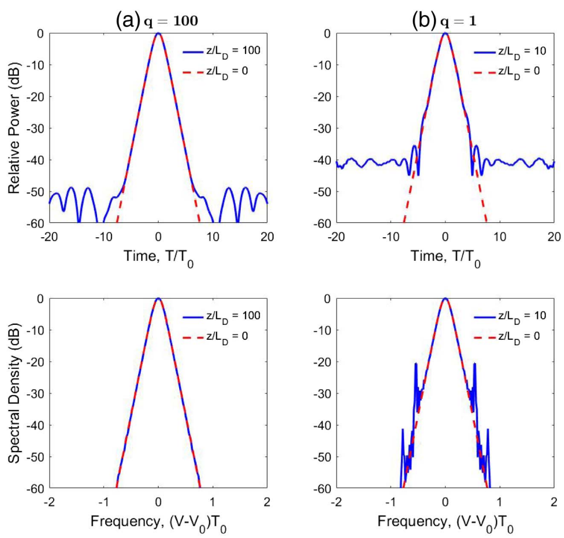

Fig. 2. Comparison of temporal (top) and spectral (bottom) intensity profiles for a fundamental GRIN soliton in the two cases shown in Fig. 1.

z and maintains its initial value. In this situation, GRIN solitons reduce to "bullet-like" spatiotemporal solitons whose size and shape remain fixed both in space and time as they propagate along the fiber. When C is close to 1, GRIN solitons are not perturbed much by weak spatial oscillations and can remain stable over very long lengths if $q \gg 1$. When C deviates from 1 by a factor of up to 5, we recover the situation shown in Figs. 1 and 2. When C deviates from 1 by a larger factor, perturbations induced by beam width oscillations become larger and limit the fiber length over which GRIN solitons remain stable.

The standard NLS equation supports a whole family of solitons [3] classified through their soliton order N. Since Eq. (10) has the same mathematical form, we expect the modified parameter $\bar{N}$ to play the same role. Thus, higher order GRIN solitons must form for integer values of $\bar{N} > 1$. Here, we investigate the stability of such solitons by solving Eq. (8) numerically. Figure 3 shows the evolution of a third-order soliton over $10L_D$ by keeping all parameters the same as in Fig. 1 and setting $\bar{N} = 3$ in Eq. (11). In the case of $q = 100$, higher order GRIN solitons exhibit a periodic evolution pattern such that the original shape and spectrum are recovered at distances $\xi = m\pi/2$, indicating that the soliton period is $(\pi/2)L_D$. This is expected from standard soliton theory [3]. From our earlier discussion, we expect this periodic evolution to become unstable as q becomes close to 1. Indeed, as seen in Fig. 3(b), the periodic evolution breaks down just after one dispersion length in the case of $q = 1$.

Since short pulses are often used in experiments, we briefly examine the impact of third-order dispersion (TOD) on a fundamental GRIN soliton. Similar to the case of standard solitons, we keep one additional term in the expansion of the dispersion operator such that $\hat{D}(\omega) = \beta_2\omega^2/2 + \beta_3\omega^3/6$, where β_3 is the TOD parameter. As a result, the normalized NLS Eq. (8) has an additional third derivative term and takes the form

$$i\frac{\partial U}{\partial \xi} + \frac{1}{2}\frac{\partial^2 U}{\partial \tau^2} - i\delta\frac{\partial^3 U}{\partial \tau^3} + N^2 f^{-1}(\xi)|U|^2 U = 0, \qquad \textbf{(12)}$$

where the dimensionless parameter $\delta = \beta_3/(6|\beta_2|T_0)$ accounts for the TOD. As before, we solve this equation numerically using $\bar{N} = 1$ and 3 with $\delta = 0.1$. Figure 4 shows the evolution over $5L_D$ by keeping all other parameters the same as in Fig. 1(a). In the case of $\bar{N} = 1$, the soliton develops an

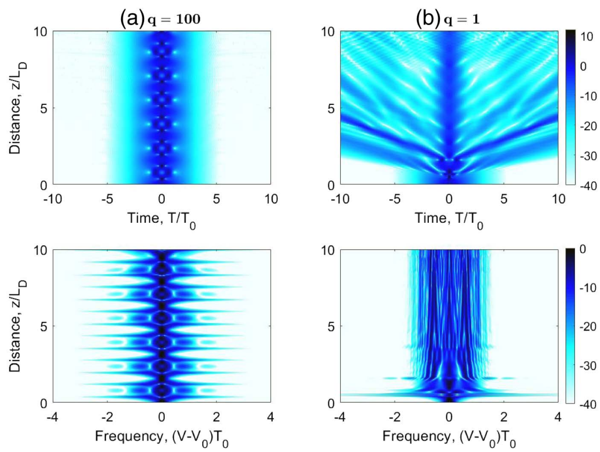

Fig. 3. Same as Fig. 1 except that evolution of a third-order GRIN soliton ($\bar{N} = 3$) is shown for the same two values of q.

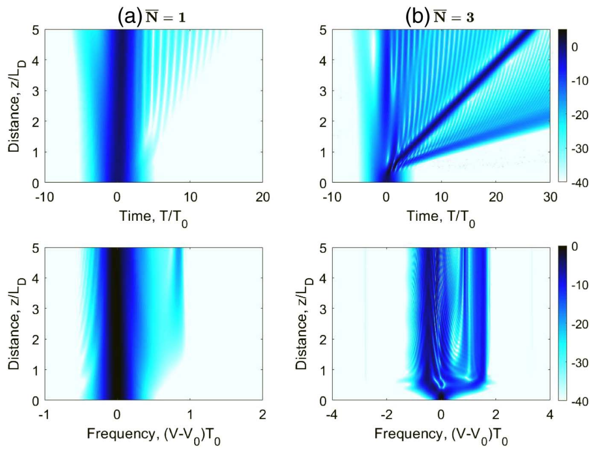

Fig. 4. Effect of TOD on soliton evolution for (a) $\bar{N} = 1$ and (b) $\bar{N} = 3$ for the parameter values used in Fig. 1(a).

oscillating tail on the trailing side. This can be interpreted as the radiation shed by a fundamental GRIN soliton in the form of a dispersive wave because of TOD-induced perturbations [18]. The appearance of a new spectral peak with a frequency shift near $(\nu - \nu_0)T_0 = 0.8$ supports this interpretation. Indeed, the position of this peaks agrees with the well-known phase-matching condition [3] $\nu - \nu_0 = (4\pi\delta T_0)^{-1}$. In the case of $\bar{N} = 3$, the evolution seen in Fig. 4(b) can be interpreted as the fission of a third-order soliton, resulting in three shorter fundamental solitons that also shed radiation as dispersive waves. This scenario is identical to that of standard perturbed solitons and leads to supercontinuum generation.

In conclusion, we have presented a new method, to the best of our knowledge, that can be used to study the stability of multimode solitons in GRIN fibers. Rather than employing a modal approach, a variational method is used to find an approximate solution of the full problem in the form of a pulsed Gaussian beam. The periodic self-imaging of the Gaussian beam results in a single NLS equation whose nonlinear term varies periodically along the length of a GRIN fiber. We used this equation to investigate the conditions under which temporal GRIN solitons can form inside such a fiber. Using the soliton units, we have identified a temporal length scale L_d and a spatial length scale z_p, whose ratio q provides a dimensionless quantity that can be used to find the conditions under which fundamental and higher order solitons can form and propagate stably inside a GRIN fiber. The most important condition is that $q = L_D/z_p$ should be a large number exceeding 10. We showed that when this condition is satisfied, the nonlinear term can be averaged over one spatial period z_P, and the problem reduces to a standard NLS equation with a modified soliton parameter $\bar{N}$. The fundamental GRIN solitons form for $\bar{N} = 1$, and higher order solitons exist for other integer value of $\bar{N}$.

We investigated stability of optical solitons in GRIN fibers by solving numerically the underlying $(1 + 1)D$ NLS equation that included spatial self-imaging effects through a periodically varying nonlinear parameter. The results show that fundamental GRIN solitons can propagate stably over $100L_D$ or more when q exceeds 100. In real units, pulses as short as 100 fs can form fundamental GRIN solitons that propagate stably over distances exceeding 1 km.

One may ask how the GRIN soliton studied here is related to the multimode soliton studied in Ref. [8], where different modes shift their spectra to move in such a way that all modes forming the soliton move at a common speed. Since we do not use a modal approach, we cannot decompose the soliton's spectrum into its multiple parts associated with individual modes. However, we note that our approach is valid when the input pulse excites a large number of modes. Solitons studied in Ref. [8] using multimode equations [12] were composed of a few low-order modes; our approach cannot be used for such solitons.

One may also ask whether our solution agrees with the full $(3 + 1)D$ problem. Even though we have not done such a comparison in this Letter, we fully expect our result to agree with the full problem if the condition $z_p \ll L_D$ is satisfied. This is the condition for which spatial variations affect the temporal dynamics but the reverse does not occur, i.e., spatial oscillations of the beam are not affected much by temporal changes. It is well known that space-time coupling inherent in Eq. (2) can occur and has been observed in several experiments [19–21]. However, the $(1 + 1)D$ NLS equation used here is quite successful in predicting the observed features in its validity regime [13]. Clearly, much more work remains to be done to fully understand the regimes in which such a simple approach can be used with success.

Funding. National Science Foundation (NSF) (ECCS 1505636).

REFERENCES

1. Y. S. Kivshar and G. P. Agrawal, *Optical Solitons: From Fibers to Photonic Crystals* (Academic, 2003).
2. L. F. Mollenauer and J. P. Gordon, *Solitons in Optical Fibers: Fundamental and Applications* (Academic, 2006).
3. G. P. Agrawal, *Nonlinear Fiber Optics*, 5th ed. (Academic, 2013).
4. A. Hasegawa, Opt. Lett. **5**, 416 (1980).
5. B. Crosignani and P. Di Porto, Opt. Lett. **6**, 329 (1981).
6. S. S. Yu, C. H. Chien, Y. Lai, and J. Wang, Opt. Commun. **119**, 167 (1995).
7. S. Raghavan and G. P. Agrawal, Opt. Commun. **180**, 377 (2000).
8. W. H. Renninger and F. W. Wise, Nat. Commun. **4**, 1719 (2013).
9. L. G. Wright, W. H. Renninger, D. N. Christodoulides, and F. W. Wise, Opt. Express **23**, 3492 (2015).
10. Z. Zhu, L. G. Wright, D. N. Christodoulides, and F. W. Wise, Opt. Lett. **41**, 4819 (2016).
11. O. V. Shtyrina, M. P. Fedoruk, Y. S. Kivshar, and S. K. Turitsyn, Phys. Rev. A **97**, 013841 (2018).
12. F. Poletti and P. Horak, J. Opt. Soc. Am. B **25**, 1645 (2008).
13. M. Conforti, C. M. Arabi, A. Mussot, and A. Kudlinski, Opt. Lett. **42**, 4004 (2017).
14. M. Karlsson, D. Anderson, and M. Desaix, Opt. Lett. **17**, 22 (1992).
15. S. Longhi and D. Janner, J. Opt. B **6**, S303 (2004).
16. A. Hasegawa and Y. Kodama, Opt. Lett. **15**, 1443 (1990).
17. G. P. Agrawal, *Fiber-Optic Communication Systems*, 4th ed. (Wiley, 2013).
18. P. K. A. Wai, H. H. Chen, and Y. C. Lee, Phys. Rev. A **41**, 426 (1990).
19. L. G. Wright, D. N. Christodoulides, and F. W. Wise, Nat. Photonics **9**, 306 (2015).
20. G. Lopez-Galmiche, Z. Sanjabi Eznaveh, M. A. Eftekhar, J. Antonio Lopez, L. G. Wright, F. Wise, D. Christodoulides, and R. Amezcua Correa, Opt. Lett. **41**, 2553 (2016).
21. K. Krupa, C. Louot, V. Couderc, M. Fabert, R. Guenard, B. M. Shalaby, A. Tonello, D. Pagnoux, P. Leproux, A. Bendahmane, R. Dupiol, G. Millot, and S. Wabnitz, Opt. Lett. **41**, 5785 (2016).